Classical Antiferromagnet on a Hyperkagome Lattice

John M. Hopkinson,[1] Sergei V. Isakov,[1] Hae-Young Kee,[1] and Yong Baek Kim[1,2]
[1]*Department of Physics, University of Toronto, Toronto, Ontario M5S 1A7, Canada*
[2]*Department of Physics, University of California, Berkeley, California 94720, USA*
(Received 8 November 2006; revised manuscript received 20 March 2007; published 19 July 2007)

Motivated by recent experiments on $Na_4Ir_3O_8$ [Y. Okamoto, M. Nohara, H. Aruga-Katori, and H. Takagi, arXiv:0705.2821 (unpublished)], we study the classical antiferromagnet on a frustrated three-dimensional lattice obtained by selectively removing one of four sites in each tetrahedron of the pyrochlore lattice. This "hyperkagome" lattice consists of corner-sharing triangles. We present the results of large-N mean field theory and Monte Carlo computations on $O(N)$ classical spin models. It is found that the classical ground states are highly degenerate. Nonetheless a nematic order emerges at low temperatures in the Heisenberg model ($N = 3$) via "order by disorder," representing the dominance of coplanar spin configurations. Implications for ongoing experiments are discussed.

DOI: 10.1103/PhysRevLett.99.037201 PACS numbers: 75.10.Hk, 75.40.Cx, 75.50.Ee

Antiferromagnets on geometrically frustrated lattices often possess macroscopically degenerate classical ground states that satisfy peculiar local constraints imposed by the underlying lattice structure [1]. Such highly degenerate systems are extremely sensitive to thermal and quantum fluctuations, and thereby intriguing classical and quantum ground states may emerge via "order by disorder" [2]. On the other hand, systems may remain disordered even at zero temperature [3]. These paramagnetic states are called spin liquid phases and their classical and quantum varieties have been recent subjects of intensive theoretical and experimental research activities [1]. Excitement in such spin systems [4] has also led to developments in mesoscopics [5], optical lattices [6], and quantum coherence and computing [7].

Among several examples of two and three-dimensional frustrated magnets, the kagome and pyrochlore lattices have obtained particular attention because a relatively large number of materials with the magnetic ions sitting on these lattice structures are available [1]. Both of these lattices are corner-sharing structures of a basic unit: the triangle and tetrahedron, respectively. Despite this similarity, the classical Heisenberg magnet orders on the kagome lattice [8,9] while it remains disordered on the pyrochlore lattice [10]. The nature of the spin-$\frac{1}{2}$ quantum Heisenberg magnets on these lattices has not been settled and remains an important open problem [11,12]. On the other hand, spin-$\frac{1}{2}$ systems are rare on these lattices and other degrees of freedom such as lattice distortions may play an important additional role. As a result, direct experimental tests on spin-$\frac{1}{2}$ quantum magnets have been difficult to realize.

In this context, the recent experiments on $Na_4Ir_3O_8$ [13] may provide an important clue on these issues, albeit in a different three-dimensional frustrated lattice. Here Ir^{4+} carries spin-$\frac{1}{2}$ as the five d electrons form a low spin state in the t_{2g} level. The Ir and Na ions together occupy the sites of the pyrochlore lattice such that only three of the four sites of each tetrahedron are occupied by Ir. The resulting lattice of magnetic Ir is a network of corner-sharing triangles as shown in Fig. 1, where each triangle is derived from different faces of the tetrahedra. In analogy to the kagome lattice in two dimensions, it is called the hyperkagome lattice. Even though the Curie-Weiss temperature is large, $\theta_W = -650$ K, the susceptibility and specific heat show no sign of magnetic ordering, nor lattice distortion, down to $T \sim |\theta_W|/200$ [13], suggesting that it may be a spin liquid down to low temperatures.

In this Letter, we study the classical antiferromagnet on the hyperkagome lattice. Such investigations not only reveal the behavior of the antiferromagnet in the classical regime, but also provide an important starting ground for the understanding of quantum fluctuation effects. We first study the large-N limit of the $O(N)$ vector spin model at zero temperature and compute the spin-spin correlation function in the large-N mean field theory [14,15]. It is found that there exist macroscopically degenerate ground states.

Then we perform large-scale Monte Carlo computations on the Ising ($N = 1$) and the Heisenberg ($N = 3$) models.

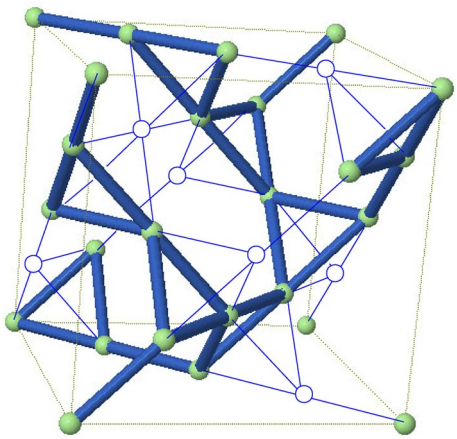

FIG. 1 (color online). The hyperkagome lattice. The thin lines show the underlying pyrochlore lattice.

The Heisenberg model (with exchange coupling J) remains disordered down to quite low temperatures, exhibiting very similar spin-spin correlations to those of the large-N model. These correlations show a characteristic dipolar structure in the reciprocal space, which can be explained by a mapping to a gauge theory [15,16]. On the other hand, the spin correlations in the Ising ($N = 1$) model turn out to be quite different.

Most interestingly, a first-order transition to a long range nematic order is observed in the Heisenberg model at a finite temperature. As explained below, this nematic order emerges via an "order by disorder" effect and represents the dominance of coplanar spin configurations. In the disordered phase no evidence of magnetic ordering is found, while our numerical data cannot definitely confirm the presence or absence of magnetic order at temperatures below the onset of nematic order. We have also investigated the effect of an external magnetic field h and found that a collinear order is chosen when $h = 2$ J in analogy to a similar study on the kagome lattice [17].

The lattice and local constraints.—The hyperkagome lattice, relevant to $Na_4Ir_3O_8$, can be represented by the simple cubic lattice with a 12-site basis, as shown in Fig. 1. This lattice is also a three-dimensional network of corner-sharing triangles. The model for the classical nearest-neighbor antiferromagnet on the hyperkagome lattice can be written as

$$H = J\sum_{\langle ij\rangle} \mathbf{S}_i \cdot \mathbf{S}_j = \frac{J}{2}\sum_{\Delta} (\mathbf{S}_\Delta)^2 + \text{const}, \qquad (1)$$

where $J > 0$, $\langle i, j\rangle$ represents the sum over the nearest neighbors, and $\mathbf{S}_i = (S_i^1, \ldots, S_i^N)$ are N-component spins of fixed length N. $\mathbf{S}_\Delta = \sum_{i\epsilon\Delta} \mathbf{S}_i$ is the vectorial sum of the spins in each triangle and $\sum_\Delta$ represents the sum over all triangles. For $N \geq 2$, the classical ground state satisfies $S_\Delta = 0$ for every triangle while the constraint on the Ising model is $S_\Delta = \pm 1$. Thus, from the outset, one may expect that the physics of the larger-N models would be different from the Ising case. This is different from the antiferromagnet on the pyrochlore lattice where the Ising and Heisenberg models satisfy the same constraint.

Large-N mean field theory.—Following Refs. [14,15], we rewrite the Hamiltonian as $H = \frac{T}{2}\sum_{i,j} M_{ij}\mathbf{S}_i \cdot \mathbf{S}_j$, where M_{ij} is the interaction matrix that has the information about the nearest-neighbor interaction. The corresponding partition function is given by $Z = \int \mathcal{D}\phi \mathcal{D}\lambda e^{-S(\phi,\lambda)}$ with the action $S(\phi, \lambda) = \sum_{i,j}[\frac{1}{2} M_{ij}\phi_i \cdot \phi_j + \frac{\lambda_i}{2}\delta_{ij}(\phi_i \cdot \phi_i - N)]$, where ϕ_i is an N-component real vector field and λ_i the Lagrange multiplier for the constraint $\phi_i \cdot \phi_i = N$.

Now we take the $N \to \infty$ limit and set a uniform $\lambda_i = \lambda_0$. The locations $i = (l, \mu)$ of spins can be labeled by those of the cubic unit cell $l = 1, \ldots, n_c$ and the lattice sites $\mu = 1, \ldots, 12$ within the unit cell (n_c is the total number of the unit cells in the lattice). The Fourier transform with respect to the positions of the unit cells leads to $S = \sum_{\mathbf{q}} \sum_{\mu,\nu} \frac{1}{2} A_{\mathbf{q}}^{\mu\nu} \phi_{\mathbf{q},\mu} \cdot \phi_{\mathbf{q},\nu}$ with $A_{\mathbf{q}}^{\mu\nu} = M_{\mathbf{q}}^{\mu\nu} + \delta_{\mu\nu}\lambda_0$. Here λ_0 and the eigenvalues $m_{\mathbf{q},\rho}$ of the 12×12 interaction matrix $M_{\mathbf{q}}^{\mu\nu}$ are determined by the saddle point equation, $12n_c = \sum_{\mathbf{q}} \sum_{\rho=1}^{12} \frac{1}{\lambda_0 + m_{\mathbf{q},\rho}}$.

It is found that the lowest eigenvalue is fourfold degenerate and independent of the wave vector. The next lowest eigenvalue has a dispersion and becomes the same as the lowest eigenvalue only at $q = 0$. These features are very similar to those in the kagome and pyrochlore lattices. These results imply that the spin structure of this system is indeed highly frustrated and that magnetic order is suppressed. The static spin-spin correlation function can be computed via [14,15] $\langle \mathbf{S}_{\mathbf{q},\mu} \cdot \mathbf{S}_{-\mathbf{q},\nu}\rangle = \sum_{\rho=1}^{12}[(U_{\mathbf{q},\mu\rho} U_{-\mathbf{q},\nu\rho})/(\lambda_0 + m_{\mathbf{q},\rho})]$, where $U_{\mathbf{q},\mu\rho}$ is a unitary transformation that diagonalizes the interaction matrix $M_{\mathbf{q}}^{\mu\nu}$. At zero temperature, the four degenerate eigenvalues dominate the behavior of the spin-spin correlation function. The resulting zero temperature structure factor, $S(\mathbf{q}) = \sum_{\mu\nu} \langle \mathbf{S}_{\mathbf{q},\mu} \cdot \mathbf{S}_{-\mathbf{q},\nu}\rangle$, in the $[hhl]$ plane of the reciprocal space is shown in Fig. 2. The presence of high intensity along bow-tie structures is apparent and qualitatively similar to that found on the pyrochlore lattice. As discussed below, the structure factor in the large-N limit is very similar to that found by Monte Carlo simulation for the Heisenberg model ($N = 3$) above the nematic ordering transition temperature, but quite different from the Ising ($N = 1$) case.

Dipolar spin correlations.—We found that the real space spin-spin correlation function at long distances is well described by the following dipolar form:

$$\langle S_i^\alpha S_j^\beta\rangle \propto \delta_{\alpha\beta}\left[\frac{3(\mathbf{e}_i \cdot \mathbf{r}_{ij})(\mathbf{e}_j \cdot \mathbf{r}_{ij})}{|\mathbf{r}_{ij}|^5} - \frac{\mathbf{e}_i \cdot \mathbf{e}_j}{|\mathbf{r}_{ij}|^3}\right], \qquad (2)$$

where $\mathbf{r}_{ij}$ is a vector connecting sites i and j, and $\alpha, \beta = x$, y, z. The "dipolar vectors" $\mathbf{e}_i$ are shown in Fig. 3.

In analogy to the pyrochlore [15], we may understand the spin correlations in this system by mapping to a pure Maxwellian action with a "Gauss law" constraint. We first consider a dual lattice of the hyperkagome lattice; the sites on the hyperkagome lattice should be placed on the bonds

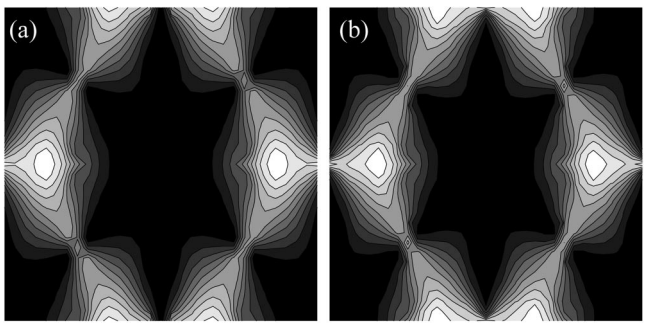

FIG. 2. Contour plots of the structure factor in the $[hhl]$ plane. (a) large-N theory at zero temperature. (b) Monte Carlo simulations at $T/J = 1/100$ and $L = 8$. Axes range from -4π to 4π and both plots are at the same resolution.

of the dual lattice. This dual lattice can be obtained by connecting centers of the tetrahedra of the underlying pyrochlore lattice, but only along the directions that would pass through the sites of the hyperkagome lattice. Then there exists a unique bond κ (on the dual lattice) for a given site i. Let us define $\mathbf{e}'_\kappa$ as the unit vector along the bond κ (see Fig. 3). We now define N number of "magnetic" vector fields $\mathbf{b}^\alpha_\kappa$ along the bond κ via $\mathbf{b}^\alpha_\kappa = S^\alpha_\kappa \mathbf{e}_\kappa$, where S^α_κ and $\mathbf{e}_\kappa$ represent the spin and unit vector defined earlier on the hyperkagome lattice. Notice that the direction of these magnetic vector fields is not along $\mathbf{e}'_\kappa$. Nonetheless the magnetic vector fields satisfy Div $\mathbf{b}^\alpha = \sum_\kappa \mathbf{e}'_\kappa \cdot \mathbf{b}^\alpha_\kappa = \sum_\kappa \mathbf{e}'_\kappa \cdot \mathbf{e}_\kappa S^\alpha_\kappa = 0$ on the dual lattice. This is a direct consequence of the constraint $\sum_{i\epsilon\Delta} S^\alpha_i = 0$ and $\mathbf{e}'_\kappa \cdot \mathbf{e}_\kappa = \sqrt{2/3}$ for all κ.

We now define coarse-grained magnetic vector fields, B^α, averaged over clusters of spins [15,16]. There exist many "flippable" spin configurations where local rearrangement of the spins in a cluster can be made without violating the constraints. The coarse-grained field over such flippable spin configurations will average out to a small value. Then the large entropic weight is related to the small values of B^α. This feature can be represented by an entropic weight of the form $\exp(-\frac{K}{2}\int d\mathbf{r}\mathbf{B}^2)$ [15,16]. This Maxwellian form of the "action" and the "Gauss law" constraint will lead to the dipolar form of $\langle B^\alpha_i(\mathbf{r}) B^\beta_j(0)\rangle \propto \delta_{\alpha\beta}(3x_i x_j - r^2\delta_{ij})/r^5$, and hence the spin-spin correlation function in Eq. (2). The discovery of such spin correlations supports the entropic argument *a posteriori*.

Monte Carlo simulations.—Classical Monte Carlo simulations for the Heisenberg ($N = 3$) and Ising ($N = 1$) models are performed on $L \times L \times L$ clusters of unit cells. We mostly discuss the results of the Heisenberg model here and mention those of the Ising model only as necessary. In the first place, a first-order transition occurs in the Heisenberg model. This can be most clearly seen in the nematic correlation function defined as [8]

$$g(\mathbf{r}_a - \mathbf{r}_b) = \tfrac{3}{2}\langle(\mathbf{n}_a \cdot \mathbf{n}_b)^2\rangle - \tfrac{1}{2}, \qquad (3)$$

and $\mathbf{n}_a = [2/(3\sqrt{3})](\mathbf{S}_1 \times \mathbf{S}_2 + \mathbf{S}_2 \times \mathbf{S}_3 + \mathbf{S}_3 \times \mathbf{S}_1)$,

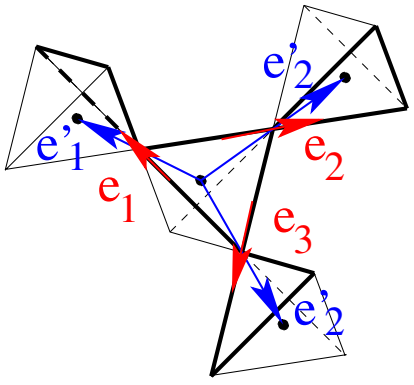

FIG. 3 (color online). The dipolar ($\mathbf{e}_\kappa$) and dual lattice ($\mathbf{e}'_\kappa$) vectors.

where $\mathbf{S}_1$, $\mathbf{S}_2$, and $\mathbf{S}_3$ are three spins on the triangle a. $g(\mathbf{r}) = 1$ in an ideal coplanar state and $g(\mathbf{r}) = 0$ in a noncoplanar state. The nematic correlation function for the next-nearest-neighbors is shown in Fig. 4 and it clearly shows a first-order transition from a low temperature nematic ordered state to a disordered state. Hysteresis associated to this transition occurs in the temperature window $(1 - 5) \times 10^{-3}$ J; coplanar configurations are chosen below this window via "order by disorder." Similar behavior is seen for the nearest-neighbor and all higher-neighbor correlations. The energy and specific heat data are also consistent with the first-order transition to nematic order (see Fig. 5). Notice that the Monte Carlo data for the three largest system sizes $L = 6$, 8, and 9 are almost identical. The zero temperature specific heat approaches 11/12 per spin, which is consistent with the expectation that the low temperature phase is dominated by coplanar spin structures. Analysis about coplanar states tells us that there are 4 quartic and 20 quadratic modes per unit cell. Since each quartic (quadratic) mode contributes 1/4(1/2) to the specific heat [8], the total specific heat becomes 11/12 per spin. Interestingly the same zero temperature specific heat was obtained in the Heisenberg model on the kagome lattice [8]. The crucial difference between two cases, however, is that the nematic order on the hyperkagome lattice is long-ranged at finite temperatures while it becomes long-ranged only in the $T \to 0$ limit on the kagome lattice [8].

On the other hand, no magnetic order is seen prior to nematic order as we do not find any elastic peaks in the spin structure factor. We cannot, however, reliably comment whether there is a magnetic ordering or not at still lower temperatures.

The spin correlations in the Heisenberg model in the disordered phase are very similar to those in the large-N mean field theory (see Fig. 2) and can be fitted to the

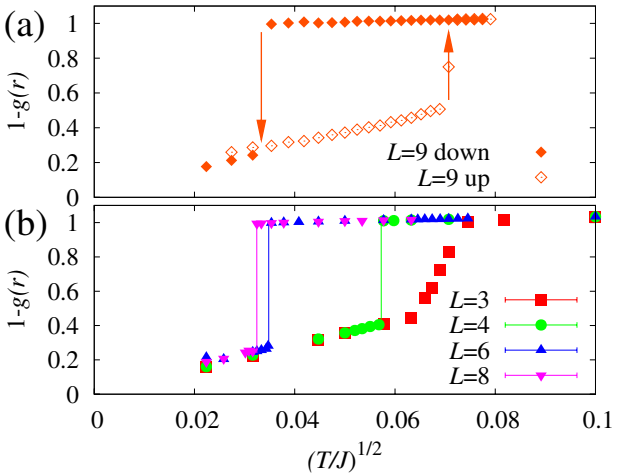

FIG. 4 (color online). The nematic correlation function for the next-nearest-neighbor triangles. (a) Hysteresis is observed upon lowering (down) or raising (up) the temperature; (b) finite size effects scale to a finite first-order transition temperature (lines guide the eye).

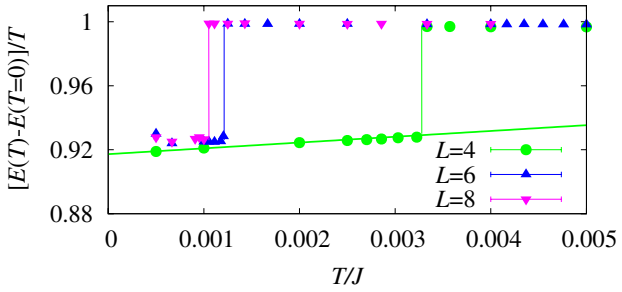

FIG. 5 (color online). The energy $E(T) - E(T = 0)$ per spin divided by temperature. In the $T \to 0$ limit, this quantity approaches $11/12$ and equals the specific heat.

dipolar form in Eq. (2). On the other hand, the results on the Ising model are markedly different; the spin-spin correlation function decays exponentially. We expect this is due to the different form of the local constraint in the Ising model.

Magnetization and susceptibility in an external field.—The magnetization as a function of an external magnetic field h is computed by the Monte Carlo simulations on the Heisenberg model. At finite temperatures, a weak plateau develops at $h/J = 2$, which leads to a singular structure in the susceptibility (not shown). This can be explained by the occurrence of a collinear order (up-up-down spin structure) by disorder at $h/J = 2$ in analogy to the kagome lattice case [17].

Implications for experiments.—A Curie-Weiss fit to the Monte Carlo susceptibility data for $T \gtrsim J$ leads to $\theta_{\mathrm{CW}} = -2.303(5)$ J (see Fig. 6). Comparing this with the experimental value $\theta_{\mathrm{CW}} = -650$ K [13], one obtains $J \approx 280$ K. This suggests that the nematic transition may occur around 0.3–1.5 K if our results are taken seriously, and below this temperature coplanar spin configurations would be preferred. Even though our classical computations may not be directly applicable at such low temperatures, we suspect that coplanar spin configurations may still dominate at low temperatures even in the quantum regime [18].

Our results also suggest that the spin correlations at $T > J/100 \sim 2$–3 K may be dominated by the physics of the classical spin liquid with dipolar spin correlations; this will be checked by neutron scattering experiments. Notice that

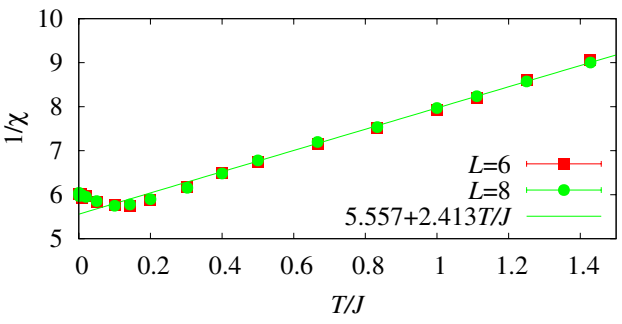

FIG. 6 (color online). The inverse susceptibility as a function of temperature, fit to a Curie-Weiss form for $T/J = 0.9$–2.0.

there is no sign of magnetic ordering down to 2–3 K in the experiment [13]; this may also be consistent with our Monte Carlo results that show no evidence of magnetic ordering above the nematic transition. It remains to be seen whether the system develops magnetic order at very low temperatures by "order by disorder" due to classical or quantum fluctuations or prefers a magnetically disordered quantum spin liquid. Finally, in the current work, we have not considered the orbital degree of freedom which may play an important role in the real material. Studies of quantum spin models and the role of orbital degrees of freedom, therefore, are important subjects of future study.

We are grateful to Hide Takagi for showing us his unpublished experimental data. We thank A. Paramekanti, M. Lawler, and especially A. Vishwanath for helpful discussions. This work was supported by the NSERC, CRC, CIAR (J. M. H., S. V. I., H. Y. K., Y. B. K.), the Sloan Foundation (H. Y. K.), No. KRF-2005-070-C00044, and the Miller Institute of Basic Research in Science at UC Berkeley (Y. B. K.).

[1] For an introductory review, see R. Moessner, Can. J. Phys. **79**, 1283 (2001).
[2] J. Villain *et al.*, J. Phys. (Paris) **41**, 1263 (1980).
[3] P. Fazekas and P. W. Anderson, Philos. Mag. **30**, 423 (1974).
[4] J. S. Helton *et al.*, Phys. Rev. Lett. **98**, 107204 (2007); P. Mendels *et al.*, Phys. Rev. Lett. **98**, 077204 (2007).
[5] R. F. Wang *et al.*, Nature (London) **439**, 303 (2006).
[6] M. Lowenstein, Nature Phys. **2**, 309 (2006); S. Wessel and M. Troyer, Phys. Rev. Lett. **95**, 127205 (2005).
[7] T. J. Osborne and F. Verstraete, Phys. Rev. Lett. **96**, 220503 (2006).
[8] J. T. Chalker, P. C. W. Holdsworth, and E. F. Shender, Phys. Rev. Lett. **68**, 855 (1992).
[9] D. A. Huse and A. D. Rutenberg, Phys. Rev. B **45**, 7536 (1992); J. N. Reimers and A. J. Berlinsky, Phys. Rev. B **48**, 9539 (1993); A. V. Chubukov, Phys. Rev. Lett. **69**, 832 (1992).
[10] R. Moessner and J. T. Chalker, Phys. Rev. Lett. **80**, 2929 (1998); C. L. Henley, Phys. Rev. Lett. **96**, 047201 (2006).
[11] S. Sachdev, Phys. Rev. B **45**, 12 377 (1992); P. Lecheminant *et al.*, Phys. Rev. B **56**, 2521 (1997); L. Balents, M. P. A. Fisher, and S. M. Girvin, Phys. Rev. B **65**, 224412 (2002); S. V. Isakov, Y. B. Kim, and A. Paramekanti, Phys. Rev. Lett. **97**, 207204 (2006).
[12] B. Canals and C. Lacroix, Phys. Rev. Lett. **80**, 2933 (1998); O. Tchernyshyov, R. Moessner, and S. L. Sondhi, Europhys. Lett. **73**, 278 (2006).
[13] Y. Okamoto, M. Nohara, H. Aruga-Katori, and H. Takagi, arXiv:0705.2821 (unpublished).
[14] D. A. Garanin and B. Canals, Phys. Rev. B **59**, 443 (1999).
[15] S. V. Isakov *et al.*, Phys. Rev. Lett. **93**, 167204 (2004);
[16] C. L. Henley, Phys. Rev. B **71**, 014424 (2005); D. A. Huse *et al.*, Phys. Rev. Lett. **91**, 167004 (2003).
[17] M. E. Zhitomirsky, Phys. Rev. Lett. **88**, 057204 (2002).
[18] At this time of writing, the experimental data below 2–3 K are not available.